Phenylbenzimidazole-Based New Bipolar Host Materials for Efficient Phosphorescent Organic Light-Emitting Diodes

Shin-ya Takizawa, Victor A. Montes, and Pavel Anzenbacher, Jr.*

Department of Chemistry and Center for Photochemical Sciences, Bowling Green State University, Bowling Green, Ohio 43403

Received February 18, 2009. Revised Manuscript Received April 20, 2009

Two new bipolar host materials based on a 1,3,5-tris(*N*-phenylbenzimidazol-2-yl)benzene (TPBI) core with the carbazole and diphenylamine groups were designed, synthesized, and applied in phosphorescent organic light-emitting diodes (PhOLEDs). The DFT calculations indicated desirable distribution of HOMO and LUMO densities, suggesting potential for bipolar charge transport. In addition, the electrochemical and phosphorescence studies revealed that neither the LUMO level nor the triplet energies differ significantly from the parent TPBI suggesting that the new materials would be suitable as hosts capable of both electron and hole transport and suitable for harvesting green electrophosphorescence. As a result of broader charge recombination zone resulting from the bipolar properties of new hosts, the devices with a simple architecture achieved significantly better current efficiencies of 48 and 60 cd/A (the power efficiencies of 46 and 70 lm/W), compared with a device using conventional TPBI host (19 cd/A; 21 lm/W) as well as a more complex device utilizing 4,4′,4″-tris(*N*-carbazolyl)triphenylamine (TCTA) as an exciton blocking layer.

Introduction

In the last decade, efforts have been devoted to the development of materials useful for the fabrication of organic light-emitting diodes (OLEDs).[1,2] The OLED performance was found to depend not only on the luminescence efficiency of the emissive materials but equally importantly also on the optical and semiconductor characteristics of hosts and charge-transporting materials.[2] Because of the multiplicity of factors influencing these features, molecular design of such materials is fairly complicated as it requires optimizing properties that include HOMO−LUMO levels, triplet excited states energy levels, film forming behavior, thermal stability, and suitable emission wavelength. Here, phosphorescent OLEDs (PhOLEDs) employing phosphorescent emitters doped into a proper charge transporting host material have attracted significant attention because of their high efficiencies as a consequence of the utilization of both singlet and triplet excitons.[1d] A number of approaches to realize highly efficient PhOLEDs were adopted focusing on limiting triplet−triplet annihilation,[3−5] triplet−polaron quenching due to triplet energy transfer to charged molecules,[5] or exciton dissociation at high current density or luminance.[6] These triplet quenching processes may be correlated with materials employed and device architectures used. In particular, the PhOLEDs utilizing phosphors with long triplet excited state lifetime and a narrow charge recombination zone are prone to triplet−triplet exciton quenching due to a local high density of triplet excitons.[5] This problem is further exacerbated by the relatively long diffusion of the triplet excitons.[7]

Thus, materials with balanced charge transport that can generate broad charge recombination zones are widely sought. However, with few exceptions,[8] most semiconductor host materials transport holes[9] or electrons.[10] In fact, most electron transporters also display hole-blocking properties, and most hole transporters display electron-blocking capacity. Thus, in general, in a device utilizing a hole-transporting host, the recombination zone is likely to be located close to the host-electron transport layer (ETL) interface. Similarly,

* Corresponding author. E-mail: pavel@bgsu.edu.

(1) (a) Shinar, J., Ed. *Organic Light-Emitting Devices, A Survey*; AIP Press/Springer: New York, 2003. (b) Kafafi, Z. H., Ed. *Organic Electroluminescence*; CRC Press: Boca Raton, 2005. (c) Li, Z.; Meng, H., Eds. *Organic Light-Emitting Materials and Devices*; CRC Press: Boca Raton, FL, 2007. (d) Yersin, H., Ed. *Highly Efficient OLEDs with Phosphorescent Materials*; Wiley-VCH: Weinheim, Germany, 2008.

(2) (a) Mitschke, U.; Bauerle, P. *J. Mater. Chem.* **2000**, *10*, 1471. (b) Kulkarni, A. P.; Tonzola, C. J.; Babel, A.; Jenekhe, S. A. *Chem. Mater.* **2004**, *16*, 4556. (c) Holder, E.; Langeveld, B. M. W.; Schubert, U. S. *Adv. Mater.* **2005**, *17*, 1109. (d) Shirota, Y.; Kageyama, H. *Chem. Rev.* **2007**, *107*, 953.

(3) Kepler, R. G.; Caris, J. C.; Avakian, P.; Abramson, E. *Phys. Rev. Lett.* **1963**, *10*, 400.

(4) Ern, V.; Bouchriha, H.; Fourny, J.; Delacote, G. *Solid State Commun.* **1971**, *9*, 1201.

(5) (a) Baldo, M. A.; Adachi, C.; Forrest, S. R. *Phys. Rev. B* **2000**, *62*, 10967. (b) Reineke, S.; Walzer, K.; Leo, K. *Phys. Rev. B* **2007**, *75*, 125328. (c) Reineke, S.; Schwartz, G.; Walzer, K.; Leo, K. *Appl. Phys. Lett.* **2007**, *91*, 123508.

(6) Kalinowski, J.; Stampor, W.; Mezyk, J.; Cocchi, M.; Virgili, D.; Fattori, V.; Di Marco, P. *Phys. Rev. B* **2002**, *66*, 235321.

(7) Baldo, M. A.; O'Brien, D. F.; Thompson, M. E.; Forrest, S. R. *Phys. Rev. B* **1999**, *60*, 14422.

(8) (a) Hancock, J. M.; Gifford, A. P.; Zhu, Y.; Lou, Y.; Jenekhe, S. A. *Chem. Mater.* **2006**, *18*, 4924. (b) Liao, Y.-L.; Lin, C.-Y.; Wong, K.-T.; Hou, T.-H.; Hung, W.-Y. *Org. Lett.* **2007**, *9*, 4511. (c) Lai, M.-Y.; Chen, C.-H.; Huang, W.-S.; Lin, J. T.; Ke, T.-H.; Chen, L.-Y.; Tsai, M.-H.; Wu, C.-C. *Angew. Chem., Int. Ed.* **2008**, *47*, 581. (d) Su, S.-J.; Sasabe, H.; Takeda, T.; Kido, J. *Chem. Mater.* **2008**, *20*, 1691. (e) Su, S.-J.; Gonmori, E.; Sasabe, H.; Kido, J. *Adv. Mater.* **2008**, *20*, 4189. (f) Ge, Z.; Hayakawa, T.; Ando, S.; Ueda, M.; Akiike, T.; Miyamoto, H.; Kajita, T.; Kakimoto, M. *Adv. Funct. Mater.* **2008**, *18*, 584. (g) Son, K. S.; Yahiro, M.; Imai, T.; Yoshizaki, H.; Adachi, C. *Chem. Mater.* **2008**, *20*, 4439. (h) Gao, Z. Q.; Luo, M.; Sun, X. H.; Tam, H. L.; Wong, M. S.; Mi, B. X.; Xia, P. F.; Cheah, K. W.; Chen, C. H. *Adv. Mater.* **2009**, *21*, 688.

10.1021/cm9004954 CCC: $40.75
Published on Web 05/11/2009

in the devices utilizing an electron transporting host the recombination zone would be located close to the hole-transporting layer (HTL).[11] This results in the narrow recombination zones formed in regions with a high polaron density. For this reason, materials capable of efficient transport of both holes and electrons should be able to generate broader recombination zones and steer them away from the interface with the charge-transport layers.[12] Such bipolar host materials are, however, still relatively rare[8] and frequently do not yield the highest-efficiency devices. On the other hand, the lack of such materials can be compensated for by judicious use of exciton-blocking layers (EBL), which increases the efficiency but also the complexity and potential cost of the device.

To achieve highly efficient OLEDs, numerous classes of charge transporting materials have been reported. For example, the hole-transporting materials comprise triarylamine or carbazole moieties.[13] On the other hand, the electron-transporting materials are structurally more diverse. Typical examples of them are tris(8-hydroxyquinolinato) aluminum(III) (Alq_3),[14] oxadiazole and triazole derivatives, and other nitrogen-containing electro-deficient materials.[15] Owing to its large HOMO−LUMO energy gap, 1,3,5-tris(*N*-phenylbenzimidazol-2-yl)benzene (TPBI) has been recognized as a useful electron-transporter and as a host material for fluorescent and phosphorescent dopants.[16] However, detailed investigation and optimization of the TPBI derivatives has not been reported so far. Such studies could further improve utility of TPBI and its derivatives in OLEDs, while the development of TPBI-based ambipolar transport materials and hosts could allow for substantial device architecture simplification and attendant cost reduction.[8] As a result of a broad charge recombination zone in an emitting layer, such materials would have the potential for achieving a high efficiency at low cost, thus being suitable for large area devices required, for example, for solid-state lighting.

Chart 1. Structure of the Compounds in This Work

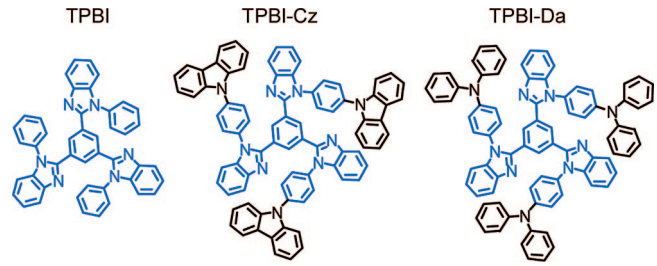

In this study, we present two bipolar transporter−host materials, TPBI-Cz and TPBI-Da (Chart 1), based on the electron-transporting TPBI core with a large HOMO−LUMO gap functionalized with hole-transporting moieties, carbazole or diphenylamine. We report on their electronic and photonic properties and the characteristics of the corresponding PhOLEDs. While the TPBI core is known to transport electrons and display high triplet energy, the carbazole[8d,9,17] and diphenylamine moieties[13] are known to impart high hole mobility, and both have been widely used in hole-transporting materials.

Results and Discussion

Theoretical Calculation. Density functional theory (DFT) calculations (B3LYP; 6-31G*) were carried out to obtain information about the HOMO and LUMO distributions of the compounds. Figure 1 depicts the resulting HOMO and LUMO of the compounds. The theoretical model indicated a significant dihedral angle (64−67°) between the *N*-phenyl ring and the benzimidazole plane in all compounds. Figure 1 shows that neither HOMO nor LUMO is localized on the *N*-phenyl ring in TPBI, suggesting that introducing the carbazolyl or diphenylamino group on the *N*-phenyl ring would not result in a significant change in the LUMO levels of the TPBI core, which would then retain proper electron-transporting properties. On the other hand, the HOMO is expected to lie on the electron-rich groups, affording an effective hole-transporting property. In fact, DFT studies of TPBI-Cz and TPBI-Da clearly indicated that their LUMOs remain on the benzene core and benzimidazole moiety with similar distributions to that of TPBI, whereas the HOMOs are localized only on the carbazole or triphenylamine part (Figure 1).

Synthesis. TPBI was prepared following the modified literature method.[18] As shown in Scheme 1, TPBI-Cz and TPBI-Da were successfully synthesized via TPBI tribromo-derivative ($TPBI\text{-}Br_3$) by using Ullmann type and palladium catalyzed reactions, respectively. $TPBI\text{-}Br_3$ was synthesized as follows. The reaction of 1-fluoro-2-nitrobenzene and 4-bromoaniline in the presence of potassium fluoride gave *N*-(4-bromophenyl)-*N*′-(2-nitrophenyl)amine in 61% yield, followed by reduction of the nitro group with stannous chloride dihydrate (80%). The resulting diamine derivative

(9) (a) Ikai, M.; Tokito, S.; Sakamoto, Y.; Suzuki, T.; Taga, Y. *Appl. Phys. Lett.* **2001**, *79*, 156. (b) Brunner, K.; Dijken, A.; Borner, H.; Bastiaansen, J. J. A.; Kiggen, N. M. M.; Langeveld, B. M. W. *J. Am. Chem. Soc.* **2004**, *126*, 6035. (c) Tsai, M.-H.; Lin, H.-W.; Su, H.-C.; Ke, T.-H.; Wu, C.-c.; Fang, F.-C.; Liao, Y.-L.; Wong, K.-T.; Wu, C.-I. *Adv. Mater.* **2006**, *18*, 1216. (d) Tsai, M.-H.; Hong, Y.-H.; Chang, C.-H.; Su, H.-C.; Wu, C.-C.; Matoliukstyte, A.; Simokaitiene, J.; Grigalevicius, S.; Grazulevicius, J. V.; Hsu, C.-P. *Adv. Mater.* **2007**, *19*, 862.
(10) Adachi, C.; Baldo, M. A.; Forrest, S. R.; Thompson, M. E. *Appl. Phys. Lett.* **2000**, *77*, 904.
(11) Adachi, C.; Baldo, M. A.; Thompson, M. E.; Forrest, S. R. *J. Appl. Phys.* **2001**, *90*, 5048.
(12) Kim, S. H.; Jang, J.; Yook, K. S.; Lee, J. Y. *Appl. Phys. Lett.* **2008**, *92*, 023513.
(13) Shirota, Y. *J. Mater. Chem.* **2000**, *10*, 1.
(14) (a) Tang, C. W.; VanSlyke, S. A. *Appl. Phys. Lett.* **1987**, *51*, 913. (b) Montes, V. A.; Pohl, R.; Shinar, J.; Anzenbacher, P., Jr. *Chem.—Eur. J.* **2006**, *12*, 4523.
(15) (a) Hughes, G.; Bryce, M. R. *J. Mater. Chem.* **2005**, *15*, 94. (b) Kim, J. H.; Yoon, D. Y.; Kim, J. W.; Kim, J.-J. *Synth. Met.* **2007**, *157*, 743.
(16) (a) Gao, Z.; Lee, C. S.; Bello, I.; Lee, S. T.; Chen, R.-M.; Luh, T.-Y.; Shi, J.; Tang, C. W. *Appl. Phys. Lett.* **1999**, *74*, 865. (b) Adachi, C.; Baldo, M. A.; Forrest, S. R.; Lamansky, S.; Thompson, M. E.; Kwong, R. C. *Appl. Phys. Lett.* **2001**, *78*, 1622. (c) Ko, C.-W.; Tao, Y.-T.; Lin, J. T.; Thomas, K. R. J. *Chem. Mater.* **2002**, *14*, 353. (d) Duan, J.-P.; Sun, P.-P.; Cheng, C.-H. *Adv. Mater.* **2003**, *15*, 224. (e) Meyer, J.; Hamwi, S.; Bulow, T.; Johannes, H.-H.; Riedl, T.; Kowalsky, W. *Appl. Phys. Lett.* **2007**, *91*, 113506-1. (f) Kim, S. H.; Jang, J.; Lee, J. Y. *Appl. Phys. Lett.* **2008**, *91*, 083511. (g) Kondakova, M. E.; Pawlik, T. D.; Young, R. H.; Giesen, D. J.; Kondakov, D. Y.; Brown, C. T.; Deaton, J. C.; Lenhard, J. R.; Klubek, K. P. *J. Appl. Phys.* **2008**, *104*, 094501.
(17) Agata, Y.; Shimizu, H.; Kido, J. *Chem. Lett.* **2007**, *36*, 316.
(18) Shi, J.; Tang, C. W.; Chen, C. T. U.S. Patent No. 5,646,948, 1997.

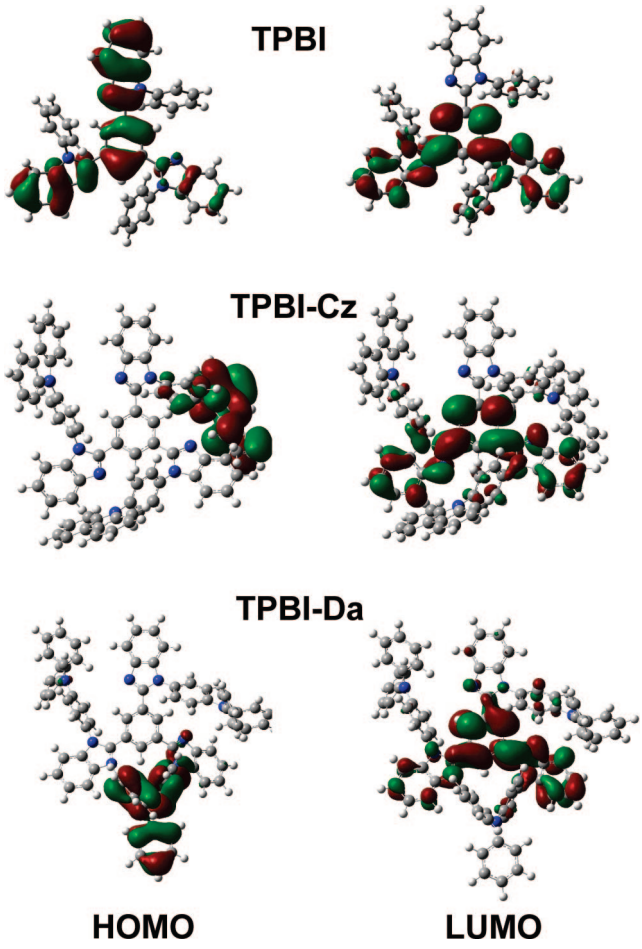

Figure 1. HOMO and LUMO distributions obtained from DFT calculations of TPBI, TPBI-Cz, and TPBI-Da.

reacted with 1,3,5-benzenetricarbonyl trichloride to produce the corresponding triamide, which was then used without purification in the next condensation reaction. Finally, TPBI-Br_3 was prepared from the trisbenzamide in 88% yield by heating at 250 °C. It should be noted that TPBI-Br_3 is a useful intermediate for introduction of many different structural features by using various coupling reactions, which are currently being explored in our laboratory.

Electrochemical Properties. Cyclic voltammetry (CV) was performed to investigate the redox behavior of the compounds. However, no clear reduction wave was observed in the potential window of the cyclic voltammograms. With respect to oxidation, only TPBI-Da underwent a reversible oxidation process while TPBI and TPBI-Cz exhibited irreversible oxidation waves. To determine the HOMO and LUMO energy levels in TPBI-Cz and TPBI-Da, the redox potentials were estimated using differential pulse voltammetry (DPV) (Table 1).[19] From the DPV data, the carbazolyl and diphenylamino groups on the *N*-phenyl ring were found to have a major effect especially on the HOMO level of TPBI. For instance, these groups negatively shifted the oxidation potential of TPBI by 0.31 and 0.63 V, respectively. On the other hand, the reduction potentials of TPBI-Cz and TPBI-Da proved to be almost identical to that of TPBI. It is noteworthy that these results are consistent with the predictions from DFT calculations, which had shown that the

Scheme 1. Synthesis of TPBI-Br_3, TPBI-Cz, and TPBI-Da[a]

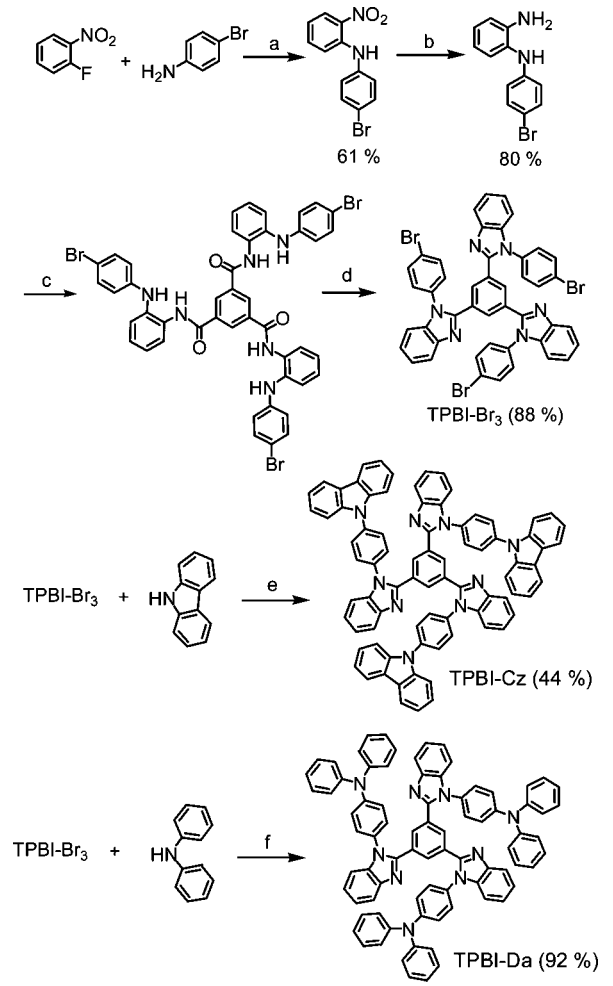

[a] Conditions: (a) KF, 170−180 °C, 72 h; (b) $SnCl_2$:$2H_2O$, EtOH, reflux, 24 h; (c) 1,3,5-benzenetricarbonyl trichloride, NMP, r.t. to 50 °C, 2.5 h; (d) 250 °C, 3 h; (e) CuI, 18-crown-6, K_2CO_3, DMPU, 210 °C, 64 h; (f) $Pd(OAc)_2$, P(*t*-Bu)$_3$, NaO^{t}Bu, toluene, 110 °C, 70 h.

LUMO energy level of TPBI-Da and TPBI-Cz remained close to that of TPBI and that all compounds had identical LUMO distributions as seen in Figure 1. In TPBI-Da, compared with TPBI-Cz, a decreased HOMO−LUMO gap was observed due to the increased HOMO level in TPBI-Da. This is presumably due to the stronger electron-donating effect of the diphenylamino group compared to that of carbazole.

Spectroscopic Studies. Table 1 summarizes photophysical data of TPBI, TPBI-Cz, and TPBI-Da. The UV−vis and PL spectra at room temperature were recorded in dichloromethane solutions (see Figure 2). The UV−vis absorption spectra of TPBI, TPBI-Cz, and TPBI-Da exhibited nearly identical absorptions at 292−303 nm attributable to the $\pi-\pi^*$ transition. However, the end absorption of TPBI-Da was red-shifted by approximately 40 nm. Interestingly, TPBI-Cz showed both the peak at 292 nm as well as a shoulder at 300 nm. This observation suggests that the *N*-phenylcarbazole moiety tilts against the benzimidazole plane and behaves

(19) In a recent paper, the HOMO and LUMO energy levels of TPBI have been reported to be−6.3 and−2.8 eV, respectively.[16e] The difference from our data may come from different measurement methods or conditions (e.g., cyclic voltammetry, differential pulse voltammetry in solution, and ultraviolet photoelectron spectroscopy in the thin film).

Table 1. Photophysical and Electrochemical Properties and HOMO−LUMO Energy Levels of the Compounds

	$\lambda_{max,abs}$, nm (ε)[a]	λ_{em} (RT), nm[a]	λ_{em} (77 K), nm[b]	τ_p, ms[c]	E_T, eV	E^{ox}, V[d]	E^{red}, V[d]	HOMO, eV	LUMO, eV	HOMO−LUMO gap, eV
TPBI	303 (5.66×10^4)	373	465; 498; 536	20.6	2.67	1.23	−2.70	−6.03	−2.10	3.93
TPBI-Cz	292 (9.35×10^4)	421	465; 498; 534	65.9	2.67	0.92	−2.65	−5.72	−2.15	3.57
TPBI-Da	301 (1.22×10^5)	474	459; 489; 523	23.2	2.70	0.60	−2.73	−5.40	−2.07	3.33

[a] In CH_2Cl_2. [b] In 2-MeTHF glass. [c] Phosphorescence lifetime. [d] Determined by DPV of 1.0 mM solutions in CH_2Cl_2 containing tetrabutylammonium perchlorate and referenced against Fc/Fc^+ (0.360 V vs $Ag/AgNO_3$).

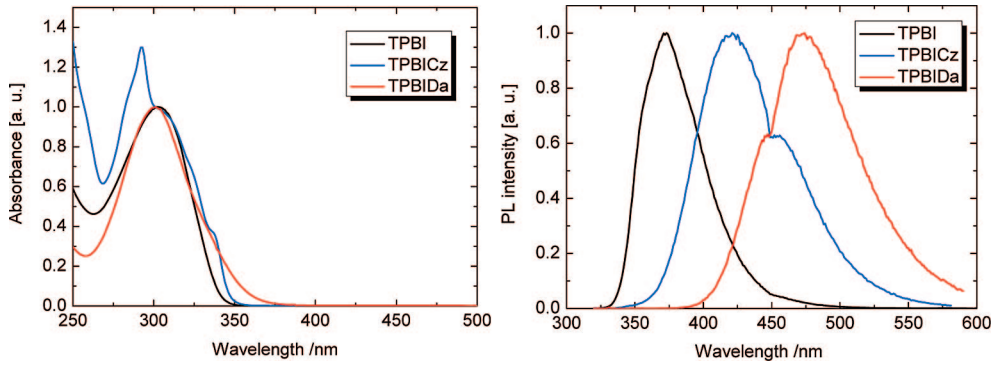

Figure 2. UV−vis absorption (left) and fluorescence spectra (right) of the compounds in CH_2Cl_2 solution.

as a fairly independent electronic entity. This is in accordance with the fact that *N*-phenylcarbazole displays a strong absorption at the same wavelength (292 nm).[15b] It also confirms the prediction that TPBI-Cz would not display strong electronic coupling between *N*-phenylcarbazole and the benzimidazole ring, thus affording the possibility of separated hole and electron-transporting functions within the molecule. This is further supported by the theoretical model from DFT calculation for TPBI-Cz, which showed the separated HOMO−LUMO distributions (Figure 1). The fluorescence spectrum of TPBI shows an emission maximum at 373 nm, while the TPBI-Cz and TPBI-Da display red-shifted maxima of 421 and 474 nm, respectively.

For host materials to yield highly efficient PhOLEDs, it is also necessary that the triplet level of the host be higher than that of the phosphorescent emitter. The high host triplet levels are essential for a high efficiency as it prevents the back energy transfer to hosts from phosphorescent dopants.[20] In the case of hosts with high triplet energy, the triplets tend to form or be trapped on the phosphorescent dopant-emitter and generate phosphorescence. The triplet energies of the hosts are obtained directly from the time-gated phosphorescence spectra recorded at 77 K. On the basis of their long lifetimes (Table 1), it was confirmed that all of the spectra correspond to the triplet excited state. The phosphorescence spectra exhibited three peaks, where TPBI showed phosphorescence 0−0 maximum at 465 nm corresponding to triplet energy of 2.67 eV, while the TPBI-Cz and TPBI-Da exhibited 0−0 transitions at 465 and 460 nm (2.67 eV, 2.70 eV). Thus, the triplet energies of TPBI-Cz and TPBI-Da are equal or higher compared to TPBI. This further confirms the hypothesis that the TPBI moiety is separated from the carbazole and diphenylamine moieties suggested by the DFT calculations. Another interesting finding is the fact that there is no direct relationship between fluorescence spectral shift and phosphorescence, that is, triplet level. This can be explained by a remarkable difference in the exchange energies, which were estimated from phosphorescence and fluorescence at 77 K ($\Delta E_{S-T} = 0.88$ eV for TPBI, 0.67 eV for TPBI-Cz, 0.38 eV for TPBI-Da). In the case of TPBI-Da, the phosphorescence appears in almost the same spectral region as fluorescence. The nature of the emissive state corresponding to the luminescence processes has been assigned to the respective singlet (τ_f 7.43 ns) and triplet (τ_p 23.2 ms) excited states using the luminescence lifetime measurements. The data above suggest that, similarly to the parent TPBI, TPBI-Cz and TPBI-Da would sufficiently confine triplet energy of green phosphorescent dopants such as iridium(III) bis(2-phenylpyridinato-*N*,$C^{2'}$)acetylacetonate [$Ir(ppy)_2(acac)$] ($E_T = 2.30$ eV)[11] and would also act as a bipolar host material for efficient green and red PhOLEDs with simplified configuration.

Phosphorescent Organic Light-Emitting Diodes. To demonstrate the ability of new TPBI-Cz and TPBI-Da host materials to confine excitons corresponding to the dopants with $E_T \leq 2.60$ eV and to test their ambipolar nature, we fabricated green PhOLEDs using the following simple three-layer configuration: indium tin oxide (ITO)/poly(ethylenedioxythiophene) doped with poly(styrenesulfonate) (PEDOT:PSS) (30 nm) was used as a hole-injection layer, followed by 4,4′-bis[*N*-(1-naphthyl)-*N*-phenylamino]biphenyl (α-NPD) (40 nm) hole-transporting layer, which was then followed by a blend of a host doped with 6% $Ir(ppy)_2(acac)$ to form the emissive layer (50 nm). The devices were finalized by deposition of CsF(1 nm)/Al(100 nm) cathode (Figure 3A). A control device using TPBI as a host and electron transport layer was also fabricated. To demonstrate the potential of the TPBI-Cz/Da materials to yield efficient devices with simpler architecture, a TPBI device with a 4,4′,4″-tris(*N*-carbazolyl)triphenylamine (TCTA) as an exciton-blocking layer (EBL) was also fabricated (Figure 3B). Table 2 summarizes the electroluminescent data of the devices.

(20) Kawamura, Y.; Goushi, K.; Brooks, J.; Brown, J. J.; Sasabe, H.; Adachi, C. *Appl. Phys. Lett.* **2005**, *86*, 071104.

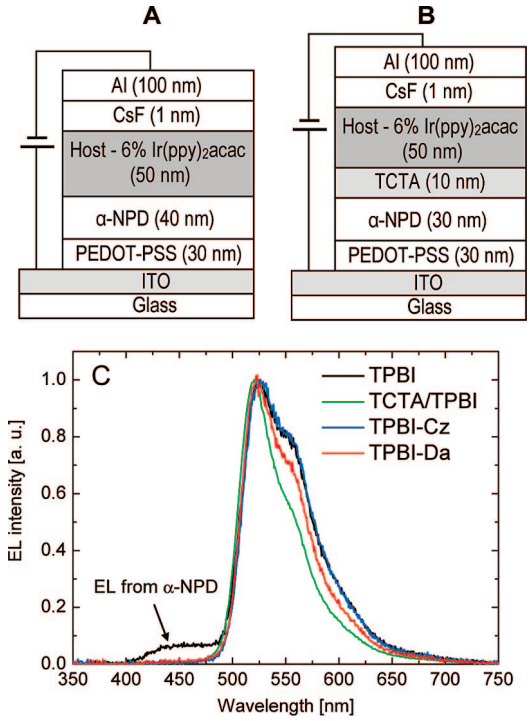

Figure 3. Panel A: Architecture of the three-layer PHOLED. Panel B: Analogous TCTA(EBL)-TPBI device. Panel C: EL spectra of the devices at 10 000 cd/m^2.

Table 2. Electroluminescence characteristics of the PhOLEDs

host	η_{ext},[a] %	η_c,[b] cd A^{-1}	η_p,[c] lm W^{-1}	L_{max},[d] cd m^{-2}	CIE[e] (x, y)
TPBI	4.7	18.8	21.0	63800	0.33, 0.58
TCTA-TPBI	5.7	26.4	33.2	78200	0.29, 0.64
TPBI-Cz	14.0	48.2	46.0	55500	0.34, 0,62
TPBI-Da	15.0	59.2	70.0	48400	0.32, 0.62

[a] External quantum efficiency (EQE, %, at 0.1 mA/cm^2). [b] Current efficiency at 0.1 mA/cm^2. [c] Power efficiency at 0.1 mA/cm^2. [d] Maximum luminance. [e] Commission Internationale de l'Eclairage coordinates at 10 000 cd/m^2.

The electroluminescence (EL) spectra recorded from devices, each comprising one of the four hosts (TPBI-only, TCTA-TPBI, TPBI-Cz, and TPBI-Da, Figure 3C), were examined. The TPBI-only device displayed α-NPD emission in the EL spectrum suggesting that the charge recombination occurs on the NPD−TPBI interface. This is likely due to low HOMO level and a low hole mobility in TPBI (see HOMO−LUMO energies in Figure 4). In the TPBI-only device we presume formation of a narrow exciton generation zone with high triplet exciton density, leading to the low EL efficiency (maximum power efficiency: 21 lm/W, current efficiency: 19 cd/A) as a result of triplet−polaron and triplet−triplet annihilation[5] as well as triplet energy loss to the adjacent α-NPD layer (E_T = 2.29 eV).[21] The incorporation of TCTA, which serves as an exciton-blocking layer owing to its high triplet energy (E_T = 2.76 eV),[8e] resulted in the disappearance of the α-NPD fluorescence and a dramatic increase in the device efficiency (33 lm/W, 26 cd/A). Presumably, this is due to the fact that despite the recombination likely to occur on the TCTA−TPBI interface, all excitons are harvested by the TPBI-Ir(ppy)$_2$(acac) layer.

(21) Goushi, K.; Kwong, R.; Brown, J. J.; Sasabe, H.; Adachi, C. *J. Appl. Phys.* **2004**, *9*, 5–7798.

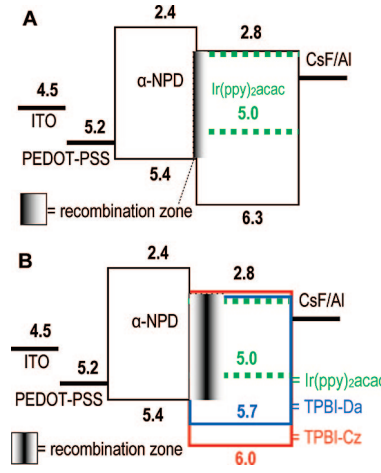

Figure 4. Energy level diagram of the PHOLEDs with TPBI (A) and TPBI-Cz and TPBI-Da (B). Plausible charge recombination−exciton generation zone is also shown. The HOMO−LUMO levels of TPBI are referenced to the values in the literature,[16e] and those of new host materials are derived from the electrochemical (DPV) data and corrected using the TPBI levels known from the literature.[16e]

Hence, the device efficiency was increased from 21 to 33 lm/W, albeit at a cost of another layer.

As expected, the simple three-layer devices (Figure 3A), both TPBI-Cz and TPBI-Da based devices, did not display α-NPD fluorescence but show a dramatic increase in the efficiency, reaching the power efficiencies of 46 and 70 lm/W at a luminance of 10 cd/m^2 (Figure 5). The comparison of the external quantum efficiencies (EQE, %, at 0.1 mA/cm^2) was also performed for the four devices (TPBI-only, TCTA-TPBI, TPBI-Cz, and TPBI-Da). Compared to the parent three-layer TPBI-only device, significant improvements in EQE were achieved in the devices with new hosts TPBI-Cz and TPBI-Da. Both the devices based on TPBI-Cz and TPBI-Da exhibited the maximum EQE in excess of 14%, whereas TPBI-only and TCTA-TPBI OLEDs displayed EQE of 4.7% and 5.7%, respectively. We presume that this is due to the formation of a more diffuse charge recombination zone located deeper in the doped TPBI-Cz/Da layer, as shown in Figure 4B. Such a diffuse zone would naturally display lower exciton density, thus decreasing the efficiency of undesirable effect such as triplet−triplet annihilation.[5] These results seem to confirm our hypothesis that the bipolar transporter hosts would increase the efficiency of the devices using simple architectures.

While the devices with new host materials exhibited a higher efficiency, it is interesting to note that a lower driving voltage was observed in the TPBI and TPBI-Da devices compared to the TPBI-Cz one. A possible explanation is that the low HOMO level of TPBI also causes charge trapping by dopant molecules adjacent to the hole-injection layer (Figure 4). On the other hand, TPBI-Da has the highest HOMO level of the three hosts facilitating the hole injection into the emissive layer and therefore is likely to display a more balanced charge transport compared to TPBI-Cz.

Comparing the data in Table 2 with the literature results on green PhOLEDs, we realized that the current and power efficiencies of these devices are among the few best in the field. In comparison, Tokito et al. have reported a four-layer device displaying power efficiency of 72 lm/W (64 cd/A)

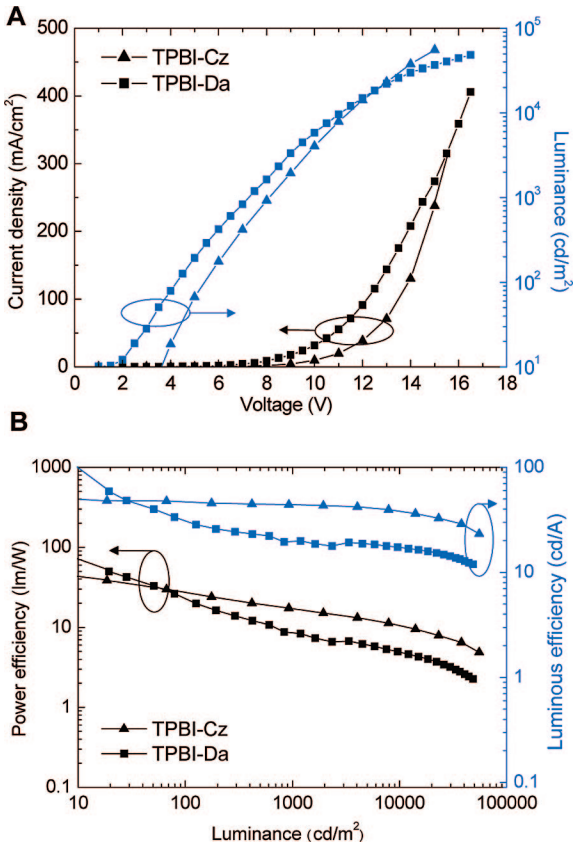

Figure 5. Panel A: Voltage–current density and voltage−luminance characteristic of the devices. Panel B: Luminance−power efficiency and luminance−luminous efficiency characteristics of the devices. The corresponding graphs that include also the reference devices are in the Supporting Information.

using the TCTA host and a new hole-exciton-blocking layer.[9a] Similarly, other groups have recently reported the efficiencies of 64 lm/W[16g] and approximately 48 lm/W[16f] with the TCTA/TPBI codeposited mixed host and the extra hole-blocking, electron-transport layers. These device architectures are still complicated, and the power efficiencies are lower compared to the data obtained for TPBI-Cz/Da devices. In this study, we could achieve the maximum current efficiencies of 48 and 60 cd/A (the power efficiencies of 46 and 70 lm/W) from three-layer devices with TPBI-Cz and TPBI-Da host. This is one of the few PhOLEDs with less than four organic layers[22] that show current efficiency exceeding 55 cd/A while most of the two or three-layer devices show a lower efficiency.[8h,16b,e,23] This suggests that the utilization of new TPBI-based bipolar hosts provides a great opportunity for fabrication of low-cost devices with reasonably high efficiency.

Conclusion

New bipolar host materials based on 1,3,5-tris(*N*-phenylbenzimidazol-2-yl)benzene (TPBI) with attached carbazole and diphenylamine groups were designed and synthesized. The DFT calculations suggested desirable distribution of HOMO and LUMO densities, suggesting potential for bipolar charge transport. The electrochemistry and UV−vis spectroscopy was then used to estimate the actual HOMO and LUMO levels, which showed a good match with the data obtained from DFT calculations. Here, the electrochemical and phosphorescence studies revealed that neither the LUMO level nor the triplet energies differ significantly from the parent TPBI suggesting that the new materials would be suitable as hosts capable of both electron and hole transport and suitable for harvesting green electrophosphorescence. The green phosphorescent OLEDs with a simple three layer architecture using these new host materials achieved significantly better efficiency of 46 and 70 lm/W at a luminance of 10 cd/m^2 compared with devices using TPBI host as well as a more complex device utilizing TCTA exciton blocking layer. As a result of their high power efficiency and simple architectures, the new bipolar host materials might find applications in low-cost electroluminescent devices in solid-state lighting and large-area light sources. Future efforts will focus on further improvements in the charge-transport balance and application for blue-green phosphorescence, which in conjunction with an orange dopant may then be used for fabrication of low-cost white-light sources.[24]

Experimental Section

Synthesis of TPBI-Br$_3$, TPBI-Cz, and TPBI-Da. *N-(4-Bromophenyl)-N′-(2-nitrophenyl)amine.* A mixture of 1-fluoro-2-nitrobenzene (4.40 g, 31.7 mmol), 4-bromoaniline (10.9 g, 63.4 mmol), and potassium fluoride (2.30 g, 39.6 mmol) was heated at 170−180 °C for 72 h. The resulting mixture was dissolved in CH_2Cl_2 (500 mL) and washed with water (120 mL × 2) and brine (120 mL). Then, the CH_2Cl_2 solution was dried over Na_2SO_4. The filtrate was evaporated in vacuo to give a crude mixture, which was subjected to column chromatography on silica gel (solvent: CH_2Cl_2). The resulting red solid was recrystallized from EtOH to afford *N*-(4-bromophenyl)-*N′*-(2-nitrophenyl)amine as orange needles (5.7 g, 61%). ^{1}H NMR (300 MHz, $CDCl_3$, δ): 9.39 (s, 1H), 8.21 (d, J = 8.7 Hz, 1H), 7.53 (d, J = 8.7 Hz, 2H), 7.39 (t, J = 7.8 Hz, 1H), 7.14−7.21 (m, 3H), 6.81 (t, J = 7.8 Hz, 1H). ^{13}C APT NMR (75.5 MHz, $CDCl_3$, δ): 142.4 (C), 138.0 (C), 135.8 (CH), 133.7 (C), 132.8 (CH), 126.8 (CH), 125.7 (CH), 118.4 (C), 118.1 (CH), 116.0 (CH). EI-MS (*m/z*): 292 [M$^+$]. Mp 161−163 °C.

N-(4-Bromophenyl)-1,2-phenylenediamine. A suspension of *N*-(4-bromophenyl)-*N′*-(2-nitrophenyl)amine (5.70 g, 19.4 mmol) and stannous chloride dihydrate (22.0 g, 97.0 mmol) in EtOH (250 mL) was refluxed for 24 h. After the reaction, the solvent was evaporated in vacuo. Then, water (500 mL) was added to the residue, followed by neutralization with $NaHCO_3$. The resulting solution was extracted with EtOAc (300 × 3 mL), and the combined organic layers were washed with water. The EtOAc solution was dried over Na_2SO_4, and the filtrate was evaporated in vacuo to obtain the product (4.1 g, 80%). ^{1}H NMR (300 MHz, $CDCl_3$, δ): 7.28 (d, J = 9.0 Hz,

(22) (a) Ding, J.; Gao, J.; Cheng, Y.; Xie, Z.; Wang, L.; Ma, D.; Jing, X.; Wang, F. *Adv. Funct. Mater.* **2006**, *16*, 575. (b) Yang, X.; Müller, D. C.; Neher, D.; Meerholtz, K. *Adv. Mater.* **2006**, *18*, 948. (c) Haldi, A.; Domercq, B.; Kippelen, B.; Hreha, R. D.; Cho, J.-Y.; Marder, S. R. *Appl. Phys. Lett.* **2008**, *92*, 253502.

(23) (a) Lo, S.-C.; Male, N. A. H.; Markham, J. P. J.; Magennis, S. W.; Burn, P. L.; Salata, O. V.; Samuel, I. D. W. *Adv. Mater.* **2002**, *14*, 975. (b) Bera, R. N.; Cumpstey, N.; Burn, P. L.; Samuel, I. D. W. *Adv. Funct. Mater.* **2007**, *17*, 1149. (c) Wu, C.-H.; Shih, P.-I.; Shu, C.-F.; Chi, Y. *Appl. Phys. Lett.* **2008**, *92*, 233303. (d) Gao, Z. Q.; Mi, B. X.; Tam, H. L.; Cheah, K. W.; Chen, C. H.; Wong, M. S.; Lee, S. T.; Lee, C. S. *Adv. Mater.* **2008**, *20*, 774.

(24) Anzenbacher, P., Jr.; Montes, V. A.; Takizawa, S. *Appl. Phys. Lett.* **2008**, *93*, 163302.

2H), 7.01−7.10 (m, 2H), 6.73−6.82 (m, 2H), 6.60 (d, $J = 9.0$ Hz, 2H), 5.18 (s, 1H), 3.75 (s, 2H). ^{13}C APT NMR (75.5 MHz, $CDCl_3$, δ): 144.9 (C), 142.5 (C), 132.4 (CH), 128.0 (C) 126.6 (CH), 125.6 (CH), 119.5 (CH), 117.0 (CH), 116.6 (CH), 111.3 (C). EI-MS (*m*/*z*): 262 [M^+]. Mp 118−122 °C.

1,3,5-Tris[N-(4-bromophenyl)benzimidazol-2-yl]benzene (TPBI-Br$_3$). *N*-(4-bromophenyl)-1,2-phenylenediamine (1.64 g, 6.23 mmol) was dissolved in 1-methyl-2-pyrrolidinone (NMP) (7 mL). To the solution was added 1,3,5-benzenetricarbonyl trichloride (0.551 g, 2.08 mmol) portionwise under nitrogen. The reaction mixture was stirred at room temperature for 2 h, and the reaction temperature was then raised to 50 °C for an additional 30 min. After cooling, the reaction mixture was poured into cold water (50 mL). The resulting precipitates were filtered off and washed with water to give crude tribenzamide. The tribenzamide was heated at 250 °C for 3 h under nitrogen. After cooling, water (50 mL) was added to the mixture and extracted with CH_2Cl_2 (50 × 3 mL). The combined organic layers were washed with water and brine, and then dried over Na_2SO_4. Solvent of the filtrate was removed in vacuo to obtain a crude solid. 1,3,5-Tris[*N*-(4-bromophenyl)benzimidazol-2-yl]benzene was isolated by silica gel column chromatography (solvent: EtOAc) (1.63 g, 88%). ^{1}H NMR (300 MHz, $CDCl_3$, δ): 7.87 (s, 3H), 7.85 (d, $J = 7.5$ Hz, 3H), 7.60 (d, $J = 8.7$ Hz, 6H), 7.27−7.39 (m, 6H), 7.18 (d, $J = 7.4$ Hz, 3H), 7.06 (d, $J = 8.7$ Hz, 6H). ^{13}C APT NMR (75.5 MHz, $CDCl_3$, δ): 150.6 (C), 143.2 (C), 137.3 (C), 135.8 (C), 133.6 (CH), 131.3 (CH), 131.1 (C), 129.1 (CH), 124.3 (CH), 123.8 (CH), 123.0 (C), 120.6 (CH), 110.6 (CH). MALDI-TOF-MS (*m*/*z*): 893 [M + H^+]. Anal. Calcd for $C_{45}H_{27}Br_3N_6$: C, 60.63; H, 3.05; N, 9.43. Found: C, 60.71; H, 2.93; N, 9.47.

1,3,5-Tris[N-(4-carbazolylphenyl)benzimidazol-2-yl]benzene (TPBI-Cz). A mixture of 1,3,5-tris[*N*-(4-bromophenyl)benzimidazol-2-yl]benzene (0.800 g, 0.897 mmol), carbazole (0.900 g, 5.38 mmol), CuI (0.049 g, 0.256 mmol), 18-crown-6 (0.093 g, 0.352 mmol), and K_2CO_3 (1.10 g, 7.99 mmol) was heated in 1,3-dimethyl-3,4,5,6-tetrahydro-2(1*H*)-pyrimidinone (DMPU) (2 mL) at 210 °C for 64 h under nitrogen. After cooling, 1 N HCl (60 mL) was added to the reaction mixture and extracted with CH_2Cl_2 (100 × 3 mL). The combined organic layers were washed with 15% NH_4OH (100 mL), water (100 mL), and brine (100 mL). Then, the solution was dried over Na_2SO_4, and filtration followed by evaporation of solvent in vacuo gave a brown oil. TPBI-Cz was isolated by silica gel column chromatography (solvent: EtOAc/CH_2Cl_2 = 1/2) (0.490 g, 44%). ^{1}H NMR (300 MHz, $CDCl_3$, δ): 8.13 (s, 3H), 8.06 (d, $J = 7.8$ Hz, 6H), 7.91 (d, $J = 7.8$ Hz, 3H), 7.60 (d, $J = 8.7$ Hz, 6H), 7.36−7.46 (m, 15H), 7.17 (t, $J = 7.4$ Hz, 6H), 7.07 (d, $J = 8.1$ Hz, 6H), 6.84−6.98 (m, 6H). ^{13}C APT NMR (75.5 MHz, $CDCl_3$, δ): 150.5 (C), 143.3 (C), 140.7 (C), 138.3 (C), 137.1 (C), 135.5 (C), 131.4 (CH), 130.9 (C), 129.1 (CH), 129.0 (CH), 126.3 (CH), 124.3 (CH), 123.7 (CH), 123.6 (C), 120.8 (CH), 120.5 (CH), 120.5 (CH), 110.7 (CH), 109.3 (CH). MALDI-TOF-MS (*m*/*z*): 1150 [M + H^+]. Anal. Calcd for $C_{81}H_{51}N_9$: C, 84.57; H, 4.47; N, 10.96. Found: C, 84.35; H, 4.22; N, 11.13.

1,3,5-Tris[N-(4-diphenylaminophenyl)benzimidazol-2-yl]benzene (TPBI-Da). A mixture of 1,3,5-tris[*N*-(4-bromophenyl)benzimidazol-2-yl]benzene (0.500 g, 0.560 mmol), diphenylamine (0.570 g, 3.36 mmol), $Pd(OAc)_2$ (0.220 mmol), P(*t*-Bu)$_3$ (0.900 mmol), and NaO^{t}Bu (0.480 g, 4.99 mmol) in toluene (5 mL) was refluxed at 110 °C for 70 h under nitrogen. To the reaction mixture was added water (50 mL), and extraction with CH_2Cl_2 (50 × 3 mL) was performed. The combined CH_2Cl_2 layers were washed with water and dried over Na_2SO_4. The solution was filtered, and the solvent was removed in vacuo. The residue was subjected to column chromatography on silica gel (solvent: EtOAc/CH_2Cl_2 = 1/2 followed by 1/1) to afford TPBI-Da (0.598 g, 92%). ^{1}H NMR (300 MHz, $CDCl_3$, δ): 7.89−7.91 (m, 6H), 7.33−7.42 (m, 9H), 6.87−7.00 (m, 42H). ^{13}C APT NMR (75.5 MHz, $CDCl_3$, δ): 151.2 (C), 148.6 (C), 147.2 (C), 143.2 (C), 137.3 (C), 131.3 (CH), 130.7 (C), 129.9 (C), 129.5 (CH), 128.3 (CH), 124.9 (CH), 124.8 (CH), 123.8 (CH), 123.7 (CH), 123.2 (CH), 120.4 (CH), 110.8 (CH). MALDI-TOF-MS (*m*/*z*): 1156 [M + H^+]; Anal. Calcd for $C_{81}H_{57}N_9$: C, 84.13; H, 4.97; N, 10.90. Found: C, 83.76; H, 4.77; N, 10.84. None of the three compounds, TPBI, TPBI-Cz, and TPBI-Da, show clearly observable glass transition in the DSC measurement, while showing sharp peaks corresponding to the melting point.

Materials for OLED Fabrication. Poly(3,4-ethylenedioxythiophene)/poly(styrene sulfonate) (PEPOT:PSS) was purchased from H.C. Starck (Clevios P VP Al 4083). 4,4′-Bis[*N*-(1-naphthyl)-*N*-phenylamino]biphenyl (α-NPD) as a hole-transporting layer and 4,4′,4″-tris(*N*-carbazolyl)triphenylamine (TCTA) as an exciton blocking layer were purchased from H.W. Sands Corporation and Sigma-Aldrich, respectively. Iridium(III) bis(2-phenylpyridinato-*N*,$C^{2'}$)acetylacetonate [Ir(ppy)$_2$(acac)] was prepared according to the literature method.[25] All the materials including TPBI and new materials, except for PEDOT:PSS, were purified by train sublimation prior to OLED fabrication.

OLED Fabrication and Measurement. OLEDs were fabricated on glass-coated ITO substrates from Colorado Concept Coatings (150−200 nm thick, $R_\square \sim 20$ Ω/□). The ITO-coated substrates were degreased by detergent and organic solvents and then UV-ozone cleaned to increase the ITO work function. PEDOT:PSS was spin-coated over 1 × 1 in. ITO substrates at 3000 rpm and baked at 150 °C for 15 min. Organic layers were deposited at ∼0.1 nm/s in a high-vacuum chamber (10^{-7} torr, Angstrom Engineering). The electron injection buffer layer CsF (1 nm) and aluminum cathode (100 nm) were also deposited by thermal evaporation at ∼0.02 nm/s and 0.2 nm/s through a shadow mask. All the electrical and optical characterization of the diodes was performed with an integration sphere using C9920-12 External Quantum Efficiency Measurement System (Hamamatsu Photonics) and a Keithley 2400 sourcemeter. All the characterization of the devices was performed inside a nitrogen-filled glovebox.

Acknowledgment. Financial support from AFOSR (FA9550-05-1-0276 to P.A.), the State of Ohio (WCI-PVIC), and BGSU is gratefully acknowledged.

Supporting Information Available: Phosphorescence spectra of TPBI, TPBI-Cz, and TPBI-Da; figures for the device characteristics. This material is available free of charge via the Internet at http://pubs.acs.org.

CM9004954

(25) Lamansky, S.; Djurovich, P.; Murphy, D.; Abdel-Razzaq, F.; Kwong, R.; Tsyba, I.; Bortz, M.; Mui, B.; Bau, R.; Thompson, M. E. *Inorg. Chem.* **2001**, *40*, 1704.